

## Study of Nucleation-Related Phenomena in Lysozyme Solutions. Application to Gel Growth

BY MARIE C. ROBERT, YVES BERNARD AND FRANÇOISE LEFAUCHEUX

Laboratoire de Minéralogie-Cristallographie, associé au CNRS et aux Universités Paris 6 et 7,  
4 Place Jussieu, F-75252 Paris CEDEX 05, France

(Received 21 October 1993; accepted 31 January 1994)

### Abstract

Two populations of aggregates are generally identified in supersaturated solutions of biological macromolecules: small aggregates of a size which is less than 5 nm and large aggregates, the largest of which are at least one order of magnitude bigger. In order to understand the role played by the microporous network of a gel in the growth and behaviour of these different species in the prenucleation period, an *in situ* observation of nucleation has been carried out using either free solutions or solutions trapped in agarose gels. In a previous study, free solutions were investigated by small-angle neutron scattering (SANS) to identify the small aggregates. Optical observations, made under the same conditions, revealed the formation of an amorphous precipitate which disappeared at the end of the experiment. The sedimentation of this phase, which occurs in free solution but never occurs in gelled solution, depletes the solution bulk and this could explain why the nucleation density is higher in agarose gel than in free solution. The case of silica gel, the behaviour of which is completely different with respect to nucleation, will be discussed.

### 1. Introduction

Because gel growth is a particular case of solution growth, most of the usual protein crystal growth techniques can be achieved in gelled media. Since the first systematic study (Robert & Lefauchaux, 1988), this method has aroused great interest, especially for groups involved in space experiments (Miller, He & Carter, 1992). Using this technique, the solution is trapped in a microporous network, convection is prevented and growing crystals do not sedimentate. However, confining the solution in pores with a size of a few hundred nanometers may have other consequences, for example an effect on the phenomena occurring in solution during the prenucleation stage. So, after having summarized the present knowledge concerning supersaturated solutions, we will examine the results of some *in situ* observations of nucleation in free and gelled solutions in order to provide

evidence of the role played by the gel. Some experiments concerning solutions contaminated by substances acting on nucleation will be examined in parallel.

### 2. General features concerning supersaturated solutions

Numerous studies, listed below, have recently been developed to provide evidence of the species which characterize supersaturated solutions used for nucleation and crystal growth.

The first evidence that these solutions behave as a non-homogeneous medium was given by Mullin & Leci (1969); they observed the formation of concentration gradients in supersaturated solution columns of citric acid, an event which never occurs in undersaturated or just saturated solutions.

This phenomenon was observed with several materials by other authors and particularly by Myerson & Lo (1991) and Ginde & Myerson (1992) who demonstrated that such sedimentation effects agree with the hypothesis of formation of clusters containing 2–100 molecules.

The existence of such clusters had been suggested previously by measurement of diffusion coefficients in supersaturated solutions indicating a strong decrease in the values beyond saturation (Chang & Myerson, 1986). The mean cluster size is a function of several parameters such as solution age, temperature, supersaturation and thermal history of the sample. Furthermore, in a recent paper Ginde & Myerson (1992) gave a very interesting extension to their work by examining the influence of impurities on the formation of clusters and on the metastable zone width (MZW).

(i) For some materials like glycine, a given impurity (valine) used as additive causes an increase in the concentration gradient of the 'sedimentation' column, indicating an increase of the cluster size; this is correlated by enhanced nucleation (decrease of MZW).

(ii) For some other materials like potassium sulfate, addition of cobalt acetate as an impurity

decreases the concentration gradient observed and consequently the cluster size; this is correlated with inhibited nucleation (increase of the MZW).

To our knowledge, no similar 'sedimentation' studies have been performed in the case of biological macromolecules but measurements of diffusion coefficients as a function of concentration also show a decrease in coefficients beyond saturation (Mikol, Hirsch & Giegé, 1990). These measurements have been made by dynamic light scattering (DLS) which is the main technique of investigation in this domain since the pioneering work of Kam, Shore & Feher (1978).

Many other techniques have been employed recently like fluorescence anisotropy (Jullien & Crosio, 1991), small-angle X-ray scattering (SAXS) (Guilloteau, 1991), dialysis kinetics (Wilson & Pusey, 1992) or small-angle neutron scattering (SANS) (Boué, Lefauchaux, Rosenman & Robert, 1993) to study the model molecule hen egg-white (HEW) lysozyme and also a few larger molecules.

Most of the time, the results show the presence of two main populations:

(i) Small aggregates whose size is less than 5 nm which gather together less than 10 molecules.

(ii) Large aggregates which are larger by one, two or three orders of magnitude (Thibault, Langowski & Leberman, 1992; Georgalis, Zouni, Eberstein & Saenger, 1993).

For small aggregates, dialysis-kinetics techniques allow a rather direct determination of cluster size.

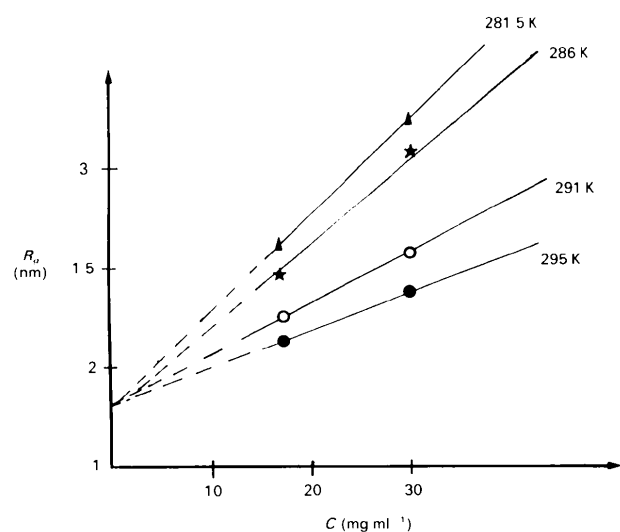


Fig. 1. Radius of gyration  $R_g$  of small aggregates determined by small-angle neutron scattering in supersaturated HEW lysozyme solutions as a function of protein concentration  $C$  at 295, 291, 286 and 281.5 K. Concentration of precipitating agent NaCl: 0.6 M. Acetate buffer solution 0.05 M in heavy water pD 4.75. Data are taken from Boué, Lefauchaux, Rosenman & Robert (1993).

SANS is a non-intrusive technique well adapted to follow the size evolution of aggregates as a function of the protein concentration. Fig. 1 shows examples of radii of gyration  $R_g$  measured in two lysozyme solutions (compositions are given in the figure caption) as a function of concentration when the temperature is lowered from 295 to 281.5 K. The  $R_g$  values lie in between the radius of a dimer (2.05 nm) and the radius of an octamer (3.20 nm).

For large aggregates, the sizes measured by DLS techniques have a very large spectra and may reach micrometer sizes, which makes them much more sensitive to sedimentation effects than small aggregates.

It is obvious that the behaviour of such aggregates must be different when the solution is trapped in a confined medium like a gel or when the solution is in a gravity-free environment.

It is interesting to consider how the formation of large and small aggregates compete during the time required to form crystal nuclei (nucleation delay). For example, the rapid formation of large aggregates which sedimentate must lead to a strong and unknown decrease in the actual supersaturation in the bulk.

These considerations lead us to follow, in real time, how nucleation proceeds in some solutions which present particularities with respect to nucleation: HEW lysozyme solutions identical to those which have been investigated by SANS (these are made with heavy water); HEW lysozyme solutions identical to the preceding ones but made with light water (these are used as a reference); HEW lysozyme solutions trapped in a light (0.05 wt%) agarose gel, knowing that agarose gels enhance the nucleation (Provost & Robert, 1991); and HEW lysozyme contaminated by traces of turkey egg-white (TEWL) lysozyme. These two lysozymes present only seven amino acids which are different over the 129 which compose the sequence. However, when the solution of one lysozyme is contaminated by the other, these differences are enough to induce significant modifications in the nucleation and growth processes (Abergel, Nesa & Fontecilla-Camps, 1991). The influence of additives upon nucleation has been thoroughly investigated in the case of inorganic compounds because of applications in industrial crystallization (Nylt, 1978). In the case of macromolecules, the study of Abergel *et al.* (1991) is, to our knowledge, the first of this type.

### 3. *In situ* observation of crystal nucleation

#### 3.1. Experimental

The set up is presented in Fig. 2. Two or three cells are illuminated by a 5 cm parallel beam emitted from

a white source. The images of the cells at different times are recorded with a CCD or a photcamera. The three cells (*C*) are identical; they are made of glass or quartz, they have the same width (1 cm) and the same thickness along the optical path (0.5 or 1 cm); they are immersed in the water bath of a thermostat equipped with windows (*W*). This thermostat is made of two envelopes; the external one (*V*), used as thermal insulator, is connected to a vacuum pump, the inner one (*L*) is connected to a water loop regulated at  $\pm 0.1$  K. A thermocouple is located at the upper part of the central cell which allows temperature recordings. A typical temperature profile is presented in Fig. 3.

The cells are filled at time  $t_0$  with equal volumes of lysozyme and salt solutions (the solutions are filtered with  $0.22 \mu\text{m}$  Millipore membranes). Mixing of the two solutions is achieved by gently rotating the cell on itself. In some cases a solution of agarose is previously added to the salt solution for further gelling of the medium; this requires handling of the different used solutions above the gelling point which is 303 K (Robert, Provost & Lefauchaux, 1992).

All the solutions are 0.05 *M* acetate buffer solutions (pH or pD 4.75) prepared with commercially available deionized and three-times distilled water (Biosedra) or with heavy water (atom% D > 99.8, Fluka). Hen egg-white (HEW) lysozyme (batch 89F8276) and turkey egg-white (TEW) lysozyme (batch 31H8255) were purchased from Sigma. The other reactants (Pro Analysis) were from Merck.

The compositions of solutions studied in four experiments, numbered (I) to (IV), are given in Table 1. They are labelled H for light-water solutions and D for heavy-water solutions. The concentration of precipitating agent NaCl is the same (0.6 *M*) for all the solutions.

Supersaturation is obtained by varying the lysozyme content and/or the temperature which is progressively lowered in steps from 295 to 281.5 K and then kept constant. Photographs are taken at regular time intervals (0.5 or 1 h).

Figs. 4, 5, 8 and 9 present sequences of cell images taken at decreasing temperatures for the four sets of

Table 1. *Composition of the solutions studied in experiments (I)–(IV)*

	HEW lysozyme (mg ml <sup>-1</sup> )	TEW lysozyme (mg ml <sup>-1</sup> )	Agarose (wt%)	Experiment
H <sub>1</sub>	30	0	0	(I)
H <sub>2</sub>	17	0	0	(I), (II)
H <sub>3</sub>	17	1.7	0	(II)
H <sub>4</sub>	17	0	0.05	(II)
D <sub>0</sub>	30	3	0	(III)
D <sub>1</sub>	30	0	0	(III)
D <sub>2</sub>	17	0	0	(III), (IV)
D <sub>3</sub>	17	1.7	0	(IV)
D <sub>4</sub>	17	0	0.05	(IV)

experiments. Some parasitic gas bubbles *b* (Figs. 4a and 5a) appear at the beginning of the experiments; they are located in the inner water bath on the windows or on the cell walls; fortunately they disappear later due to the higher solubility of gas at lower temperatures. Some other marks like X in Fig. 4 are also visible; these have been drawn on the cells for easier focusing.

### 3.2. Results

The sequences have been chosen in order to compare the influence of different parameters on modifications appearing in the solution during the pre-nucleation and nucleation periods.

It is intended to compare how nucleation proceeds in light and heavy water: (i) for two solution concentrations (experiments I and III); (ii) for contaminant-free and contaminated solutions (experiments II, III and IV); (iii) for gel-free and gelled solutions (experiments II and IV).

3.2.1. *Influence of solution concentration. Experiment I.* Fig. 4 shows a series of images taken at 281.5 K of two cells containing the solutions H<sub>1</sub> and H<sub>2</sub> (the cells are labelled by the name of the corresponding solution). These solutions are always clear and transparent and visible crystals appear at  $t_0 + 9$  h for H<sub>1</sub> and  $t_0 + 24$  h for H<sub>2</sub>. These last crystals are visible as new dots in Fig. 4(d), some of them being marked by arrows. Most of the crystals are grafted on the cell walls.

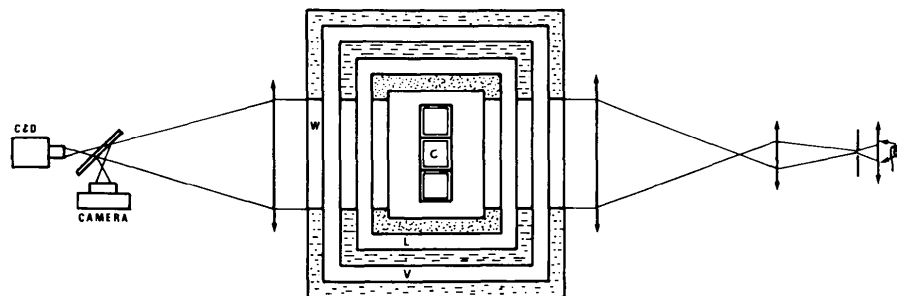


Fig. 2. Experimental set up for *in situ* observation of nucleation. The three cells *C* are inserted in a thermostat equipped with windows *W*; thermal regulation is performed by a water loop *L* isolated by vacuum *V*. The parallel beam is emitted by a white source. Images are collected on CCD or Photcamera.

*Experiment III.* Fig. 5 shows the evolution of solutions  $D_1$  and  $D_2$  undergoing the same thermal treatment as for  $H_1$  and  $H_2$ . At 291 K (Fig. 5a) both solutions are clear and transparent but around 288 K,  $D_1$  becomes opaque owing to the formation of a dense precipitate. As temperature goes down, the precipitate coarsens and the largest particles begin to sedimentate. The same phenomenon occurs for  $D_2$ , but at a lower temperature: darkening occurs around 283 K; the sedimentation is rather slow, indicating a mean particle size smaller than for  $D_1$ .

The first visible crystals appear at  $t_0 + 10$  h for  $D_1$  and  $D_2$  but their detection is made difficult, the images being blurred by the superimposed precipitate.

In both cases, crystals grow from a medium which is not perfectly clear, owing to the presence of a fine precipitate suspended in the solution. This precipitate dissolves very quickly when the supersaturation decreases: this can be evidenced in an enlarged view (Fig. 5g) of the upper part of the central cell (Fig. 5f) showing 'plumes'  $p$  surrounding the growing crystals as precipitate free zones. As a matter of fact, the solution layers close to the crystals are depleted in solute so that they are lighter than the

surrounding layers and they are driven upwards by buoyancy convection.

The fine precipitate also dissolves instantaneously as soon as the temperature is raised and photographs of cells taken at ambient temperature (Figs. 6b and 6c) only exhibit monocrystals.

Although the initial concentrations of protein are quite different in  $D_1$  and  $D_2$  cells, the number of nucleated crystals seems nearly the same: one can only notice that they are distributed more homogeneously for  $D_2$  than for  $D_1$ ; for  $D_1$ , the crystals are more numerous at the bottom than at the top.

The effects of sedimentation are reduced further by reducing the thickness of the experimental cell: Fig. 6(d) is a 1 mm thick cell which has been included in the same experiment. The growth solution is  $D_2$ , as for the 5 mm thick cell shown Fig. 4(c). The crystals are more homogeneously distributed in the thin cell.

All these observations can be understood by considering the solubility diagram (Fig. 7) in which the paths followed by solutions  $H_1$  and  $D_1$  on one side, and  $H_2$  and  $D_2$  on the other side, have been drawn.

The solid line  $S_c$  represents the solubility of HEW lysozyme in light water. A systematic study of solubility in heavy water has not been carried out in the present case but some measurements of solubility have shown that the difference between the results obtained in light and heavy water is inside the error margin (Ducruix, personal communication). Generally, the solubility of materials in heavy water is less than in light water, but in this low-solubility domain, one can consider that both representative curves merge.

A second line  $S_p$  (thick dotted line) should be taken into account; it marks a boundary beyond which amorphous precipitation occurs. As there is no precipitation lag (Feher & Kam, 1985), experiment II allows the location of two points  $A$  ( $30 \text{ mg ml}^{-1}$ , 288 K) and  $B$  ( $17 \text{ mg ml}^{-1}$ , 283 K) on this curve. These points mark the beginning of precipitation in each solution; the whole curve has been drawn by extrapolation.

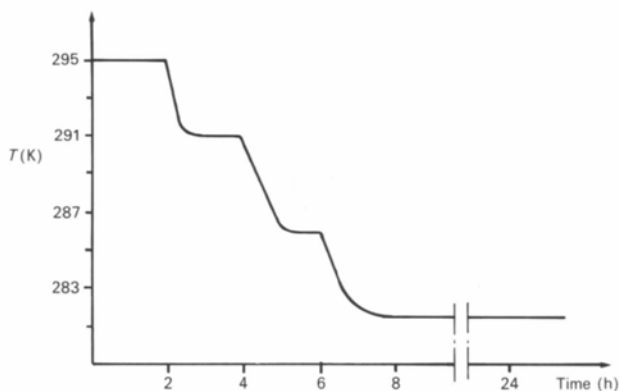


Fig. 3. Temperature profile as a function of time during the four nucleation experiments.

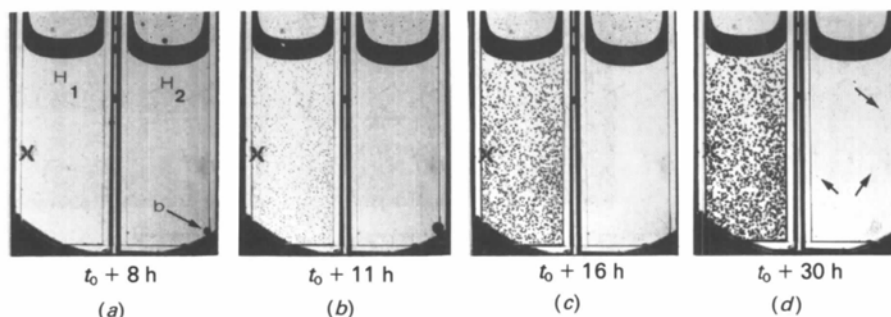


Fig. 4. (a)-(d) Sequence of images taken at 281.5 K (experiment I) showing the appearance of nucleation in light-water lysozyme solutions  $H_1$  ( $30 \text{ mg ml}^{-1}$ ) and  $H_2$  ( $17 \text{ mg ml}^{-1}$ ). Glass cells: 10 mm wide, 10 mm thick. Some new crystals appearing in  $H_2$  are marked by arrows in (d).

$T = 281.5 \text{ K}$

A third line (thin dotted line) has been drawn in the diagram: it marks the boundary beyond which amorphous precipitation might occur in light water; its location is approximated knowing first that it must be placed somewhat above  $S_p$  and second that it never intercepts the path followed by the light-water solutions  $H_1$  or  $H_2$ .

The situation exhibited in Fig. 5(b) corresponds to a point located beyond  $S_p$  for  $D_1$  and under  $S_p$  for  $D_2$ ; so the solution remains clear in  $D_2$  and a first precipitate occurs in  $D_1$ .

During the next temperature drop (Fig. 5c), precipitation intensifies in  $D_1$  and just begins in  $D_2$ . In the whole temperature domain, we are far above the solubility curve but due to an important nucleation lag, precipitation always occurs before crystallization. For a very long nucleation lag, the solute

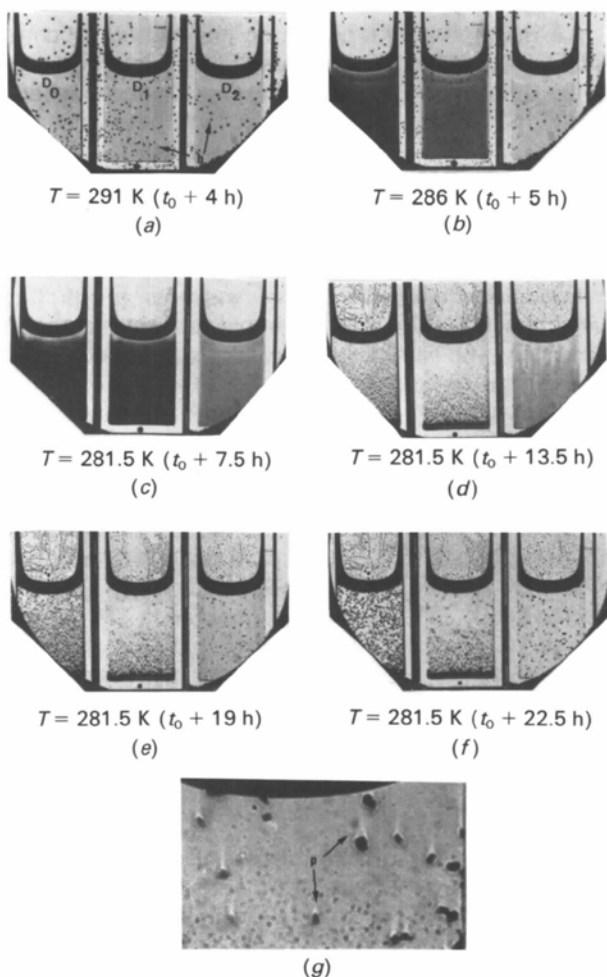


Fig. 5. (a)–(f) Sequence of images taken at decreasing temperatures (experiment III) in heavy-water lysozyme solutions  $D_0$  ( $30 \text{ mg ml}^{-1}$  contaminated by TEWL  $3 \text{ mg ml}^{-1}$ ),  $D_1$  ( $30 \text{ mg ml}^{-1}$ ) and  $D_2$  ( $17 \text{ mg ml}^{-1}$ ); *b* are parasitic gas bubbles. Quartz cells, 10 mm wide, 5 mm, thick. (g) Enlarged view of the top part of the central cell of (f).

concentrations in  $D_1$  and  $D_2$  could be nearly the same and could be represented by point *C* in the solubility diagram. This explains why the final number of crystals in both cells is not very different.

However, for larger growth times, the final size of crystals could be larger in  $D_1$  than in  $D_2$  due to the redissolution of precipitate (here we are under  $S_p$  which acts as a solute reservoir).

3.2.2. *Influence of solution contamination. Experiment II.* For light-water solutions  $H_2$  and  $H_3$  (Fig. 8), no visible differences appear during the cooling run.

*Experiments I and IV.* For heavy-water solutions, darkening occurs at the same temperature for contaminated and non-contaminated solutions with a high protein content ( $D_0$  and  $D_1$  in Fig. 5) or for a low protein content ( $D_2$  and  $D_3$  in Fig. 9). One can only note a small contrast increase for the contaminated solutions (Figs. 5*b* and 9*c*). The sedimentation effects which are specially marked at high protein content seem to be reduced for the contaminated solutions; this indicates that the presence of contaminants influences the polymerization reaction, leading to precipitates which are lighter. This

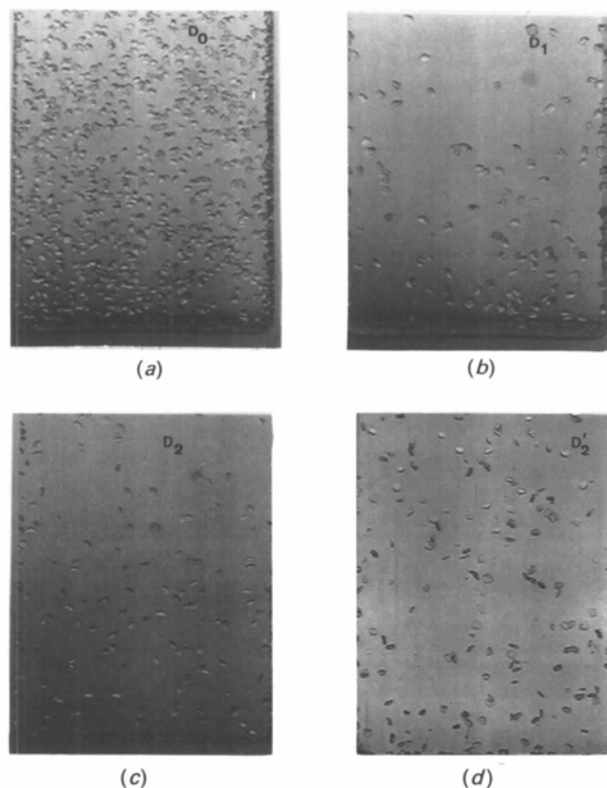


Fig. 6. (a)–(c) Optical views of cells  $D_0$ ,  $D_1$  and  $D_2$  at the end of experiment III. At room temperature the amorphous precipitate visible in Fig. 5(f) has disappeared. (d) Same experiment  $D_2'$  as for  $D_2$  except for the cell thickness which is 1 mm instead of 5 mm.

results in nucleation appearing in a medium ( $D_0$ ) which is less depleted in solute than the one ( $D_1$ ) which experiences important sedimentation effects so that the number of crystals which have nucleated in  $D_0$  is higher than in  $D_1$  (Figs. 5f, 6a, 6b).

For less concentrated solutions, we have seen that the sedimentation effects are reduced; consequently, the number of crystals obtained in  $D_2$  and  $D_3$  are about the same (Fig. 9e).

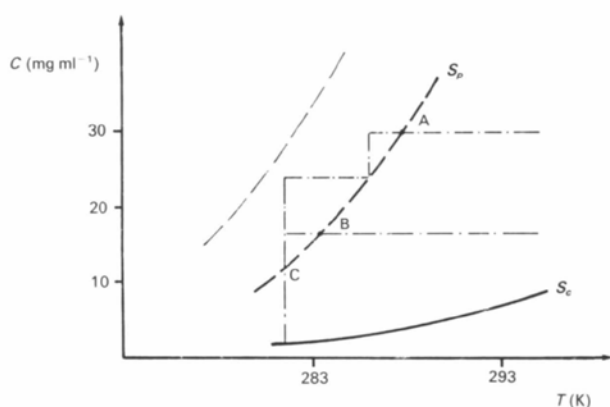


Fig. 7. Solubility diagram for HEW lysozyme in 0.05 M acetate buffer solutions pH or pD 4.75 with NaCl 0.6 M.  $C$  protein concentration,  $T$  temperature. Solid line  $S_c$  corresponds to the solubility of the crystal; the thick dotted line  $S_p$  to the solubility of precipitate for heavy-water solutions and the thin dotted line to the solubility of precipitate for light-water solutions. The paths followed by solutions  $H_1$  and  $H_2$  or  $D_1$  and  $D_2$  during the experiments are indicated.

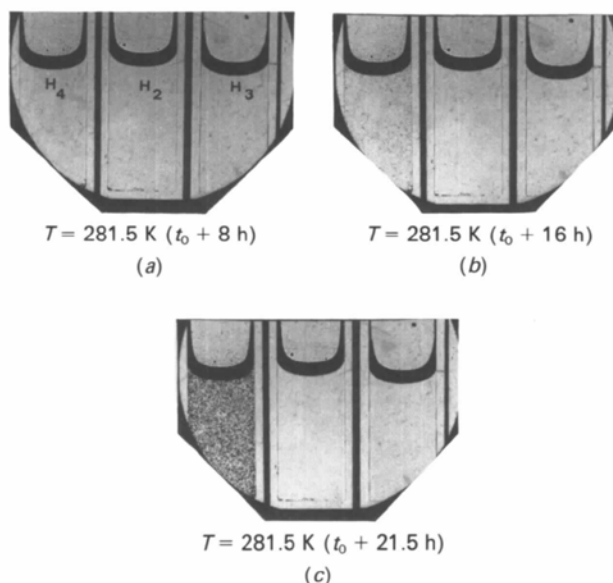


Fig. 8. (a)–(c) Sequence of images taken at 281.5 K (experiment II) in light-water HEWL solutions  $H_2$  ( $17 \text{ mg ml}^{-1}$ ),  $H_3$  ( $17 \text{ mg ml}^{-1}$  contaminated with TEWL  $1.7 \text{ mg ml}^{-1}$ ),  $H_4$  ( $17 \text{ mg ml}^{-1}$  gelled with agarose 0.05 wt%).

3.2.3. *Influence of a gel medium.* Fig. 8 presents some images of gelled ( $H_4$ ) and gel-free ( $H_2$ ) solutions containing the same protein concentration, taken at 281.5 K. No difference in the background contrast is visible but it appears that a large number of crystals nucleate and grow in the gel much earlier than in free solution. The first crystals appear there at  $t_0 + 12 \text{ h}$  instead of  $t_0 + 24 \text{ h}$ .

As for a gel-free solution at the same concentration ( $D_2$ ), darkening occurs around 283 K for a gelled solution ( $D_4$ , Fig. 9b). At the beginning, the difference in contrast between these two solutions is small but it increases very rapidly and the gelled solution becomes totally opaque (Fig. 9c). This is due to the presence of a very dense precipitate which vanishes immediately when the temperature is raised, revealing the presence of numerous well shaped crystals (Fig. 9e). The presence of agarose gel plays two roles: first it increases the rate of formation of the amorphous precipitate (and probably influences the structure of this precipitate); second, it prevents the sedimentation effects. This results in the number of crystals being higher in this gel than in free solution.

#### 4. Discussion and concluding remarks

*In situ* observations of growth media allow one to understand the role played by the 'temporary' formation of amorphous precipitates. When the precipitation is reversible, such intermediate phases cannot be detected at the end of the experiment because only monocrystals grown in a clear solution are visible.

Sedimentation of these precipitates depletes the growth solution, so that the actual supersaturation in the bulk is less than could be expected from initial conditions.

Use of gel media prevents the sedimentation and the solute is maintained in the whole volume of solution. This observation, made in the case of an agarose gel, must be valid no matter what type of gel is used because the free space in these structures (typically a few hundred nanometers large) prevents sedimentation of large aggregates. However, the nucleation properties of a physical gel like agarose are quite different from those of a chemical gel like silica gel (Provost & Robert, 1991). The former increases the nucleation rate (compared with free solution) while the second decreases the nucleation rate. For silica gel, this decrease has been interpreted by considering that this gel has a rather close porosity trapping quasi-isolated volumes of solution; when the pores are too small, they do not contain enough solute molecules to build a critical nucleus (Andreazza, Lefauchaux & Mutaftschiev, 1988). The solution is not so confined in an agarose gel whose structure is formed by entangled polysaccharide

chains. Obviously besides sedimentation effects, many other features mark the difference between free and gelled media; one can invoke, for example, chemical effects but it is surprising to observe that an addition of agarose to the growth solution has no influence on nucleation as far as the gel is not set (Provost & Robert, 1991).

Free solution growth under microgravity conditions must reduce the sedimentation effects and maintain a growth medium more homogeneous than in free solution on earth.

We have illustrated here sedimentation effects occurring during the prenucleation phase thanks to the presence of visible precipitates but one can reasonably think that the large aggregates evidenced by DLS techniques must play the same role, but as they are smaller than visible precipitates, their sedimentation times are larger.

This could be a way of understanding why microgravity conditions are beneficial for specific materials or for a given material when specific growth conditions are used, and not for the others.

It is obvious that the competition between the rates at which small and large aggregates grow must play an important role in the phenomena involved in the nucleation processes.

Understanding nucleation will require characterization of supersaturated solutions, in particular when they are trapped in different gel structures. In order to elucidate this question, many characterization techniques like DLS, SAXS and SANS might be combined to study reference materials taken in reference nucleation conditions. This is a difficult task, taking into account the requirements and limitations of each technique, but the goal is important enough to motivate a joint effort.

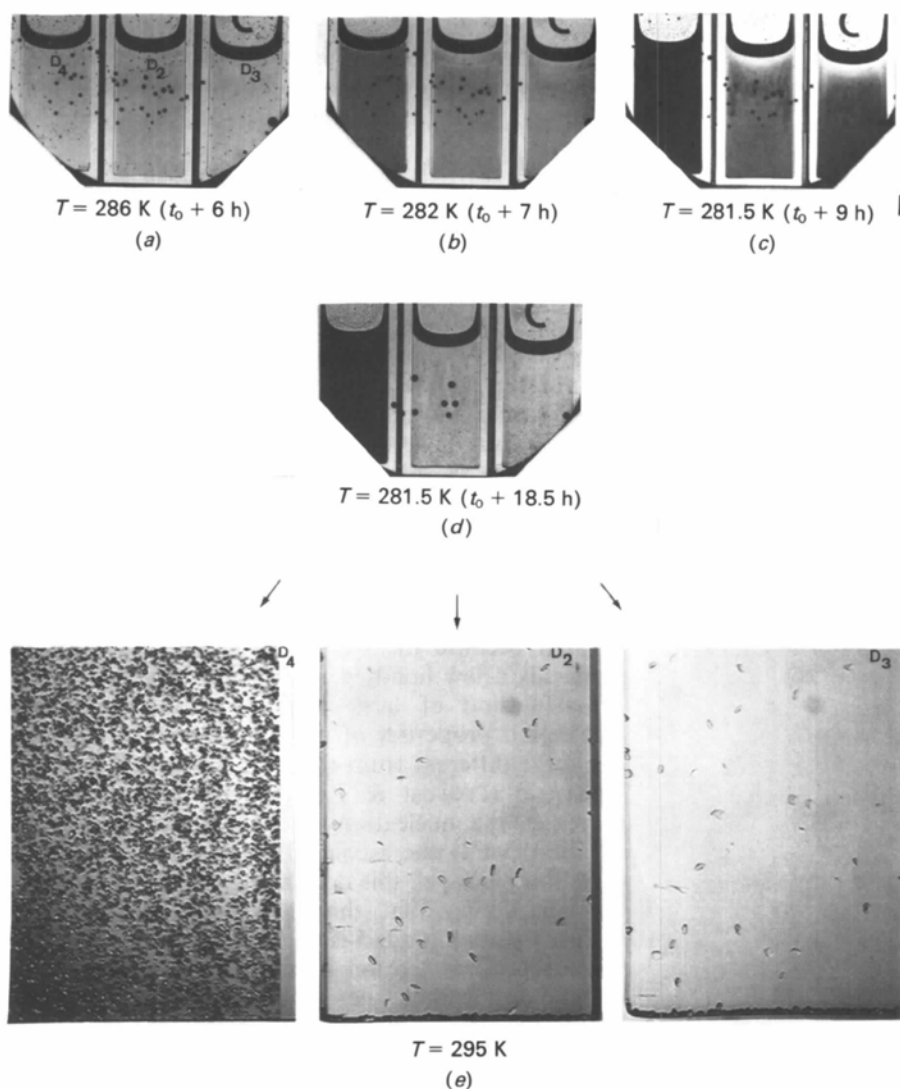


Fig. 9. (a)–(e) Sequence of images taken at decreasing temperatures (experiment IV) in heavy-water solutions D<sub>2</sub> (17 mg ml<sup>-1</sup>), D<sub>3</sub> (17 mg ml<sup>-1</sup> contaminated with 1.7 mg ml<sup>-1</sup> TEWL) and D<sub>4</sub> (17 mg ml<sup>-1</sup> gelled with agarose 0.05 wt%).

## References

- ABERGEL, C., NESA, M. P. & FONTECILLA-CAMPS, J. C. (1991). *J. Cryst. Growth*, **110**, 11–19.
- ANDREAZZA, P., LEFAUCHEUX, F. & MUTAFTSCHIEV, B. (1988). *J. Cryst. Growth*, **92**, 415–422.
- BOUÉ, F., LEFAUCHEUX, F., ROSENMAN, I. & ROBERT, M. C. (1993). *J. Cryst. Growth*, **133**, 246–254.
- CHANG, Y. C. & MYERSON, A. S. (1986). *AIChE J.* **32**, 1567–1569.
- FEHER, G. & KAM, Z. (1985). *Methods Enzymol.* **114**, 77–112.
- GEORGALIS, Y., ZOUNI, A., EBERSTEIN, W. & SAENGER, W. (1993). *J. Cryst. Growth*, **126**, 245–260.
- GINDE, R. M. & MYERSON, A. S. (1992). *J. Cryst. Growth*, **116**, 41–47.
- GUILLOTEAU, J. P. (1991). Thesis, Paris, France.
- JULLIEN, M. & CROSIO, M. P. (1991). *J. Cryst. Growth*, **110**, 182–187.
- KAM, Z., SHORE, H. B. & FEHER, G. (1978). *J. Mol. Biol.* **123**, 539–555.
- MIKOL, V., HIRSCH, E. & GIEGÉ, R. (1990). *J. Mol. Biol.* **213**, 187–195.
- MILLER, T. Y., HE, X. M. & CARTER, D. C. (1992). *J. Cryst. Growth*, **122**, 306–309.
- MULLIN, J. W. & LECI, C. L. (1969). *Philos. Mag.* **19**, 1075.
- MYERSON, A. S. & LO, P. Y. (1991). *J. Cryst. Growth*, **110**, 26–33.
- NYLT, J. (1978). *Industrial Crystallization. The Present State of the Art*, pp. 26–31. New York: Verlag Chemie.
- PROVOST, K. & ROBERT, M. C. (1991). *J. Cryst. Growth*, **110**, 258–264.
- ROBERT, M. C. & LEFAUCHEUX, F. (1988). *J. Cryst. Growth*, **90**, 358–367.
- ROBERT, M. C., PROVOST, K. & LEFAUCHEUX, F. (1992). *Crystallization of Nucleic Acids and Proteins. A Practical Approach*, edited by A. DUCRUIX & R. GIEGÉ, pp. 127–142. London: IRL Press/Oxford Univ. Press.
- THIBAUT, F., LANGOWSKI, J. & LEBERMAN, R. (1992). *J. Cryst. Growth*, **122**, 50–59.
- WILSON, L. J. & PUSEY, M. L. (1992). *J. Cryst. Growth*, **122**, 8–13.